

Signatures of single-site addressability in resonance fluorescence spectra

Peter Degenfeld-Schonburg,^{*} Elena del Valle, and Michael J. Hartmann

Physik Department, Technische Universität München, James Franck Strasse, D-85748 Garching, Germany

(Received 23 November 2011; published 27 January 2012)

Pioneering methods in recent optical-lattice experiments allow focusing laser beams down to a spot size that is comparable to the lattice constant. Inspired by this achievement, we examine the resonance fluorescence spectra of two-level atoms positioned in adjacent lattice sites and compare the case where the laser hits only one atom (single-site addressing) with cases where several atoms are illuminated. In contrast to the case where the laser hits several atoms, the spectrum for single-site addressing is no longer symmetric around the laser frequency. The shape of the spectrum of fluorescent light, therefore, can serve as a test for single-site addressing. The effects we find can be attributed to a dipole-dipole interaction between the atoms due to the mutual exchange of photons.

DOI: [10.1103/PhysRevA.85.013842](https://doi.org/10.1103/PhysRevA.85.013842)

PACS number(s): 42.50.Nn, 37.10.Jk, 42.25.Fx

I. INTRODUCTION

Over the course of the past decades, the exploration of the radiative properties of laser-driven atomic systems advanced at a stunning pace in the field of quantum optics. The fluorescence light of a coherently driven two-level atom is a common example in most textbooks [1,2]. For a coherent laser drive, the predicted Mollow spectrum is a symmetrical three-peak spectrum with a center-sideband separation given by the Rabi frequency and the detuning of the driving laser field [3–5]. Taking more than one atom into account, other interesting features of the spectrum arise due to effects of coherent and incoherent inter-atomic interactions [6]. The question to what extent the fluorescence spectrum is altered in the presence of collective effects, thus, is of great interest since it contains information about the physical setup of the atomic system [7].

In this paper, we clarify how the shape of the spectrum alters when a single atom within the atomic ensemble is addressed by an external driving field. Therefore, we compare the spectra of the situation where a laser illuminates all atoms with the situation where the laser illuminates only one atom. The usual symmetry of the spectrum breaks down if the distance between neighboring atoms is such that their dipole-dipole interaction via mutual exchange of photons is comparable to the magnitude of the driving strength.

Our investigation of the resonance fluorescence spectrum, under the assumption that single atoms in an atomic ensemble can be addressed by a laser beam, is motivated by recent experiments with optical lattices [8,9] in a Hubbard regime that traps neutral atoms in the lattice sites. High-resolution imaging systems with an optical resolution of about 600–700 nm allow resolving the fluorescent light emitted from the atoms in individual lattice sites of a two-dimensional (2D) lattice. Hence, a laser beam traveling on the same path just like the fluorescence light going through the imaging system, but in the reverse direction, can be focused onto a single site or single atom with a full width at half maximum (FWHM) of, again, 600–700 nm [10]. Such single-site addressing allows investigating local properties of quantum many-particle systems [11,12].

The origin of the effects we find for the fluorescence spectra of neutral atoms in optical lattices lies in the typical interatomic separation. On one hand, the atoms are far enough from each other to open up the possibility of single-atom addressing by focused laser beams. On the other hand, the separation is small enough so that an interatomic coupling mediated by the mutual exchange of scattered photons still influences the collective behavior. Otherwise, the fluorescence spectrum would not differ from the well-known Mollow spectrum [3].

The remainder of the paper is organized as follows. In Sec. II, we set up a master equation that describes the coupling of N two-level atoms to the quantized electromagnetic field. Due to small interatomic separations, we have to account for an effective atom-atom coupling mediated by the quantized field. The effective atom-atom coupling, namely, the dipole-dipole interaction and the collective damping rate, will be discussed in detail. We also define our notion of single-site addressing motivated by the experiment [10]. As our investigations focus on the fluorescence spectrum of the atomic ensemble, the power spectrum is introduced in Sec. III. We then present our numerical results in Sec. IV for a number of up to five two-level atoms representing single-site addressability in a one-dimensional (1D) or 2D optical lattice. In all cases, we find a broken symmetry in the fluorescence spectra if only one atom is addressed by the laser field. We demonstrate that this effect only occurs if the dipole-dipole interaction is finite. In Sec. V, we make some general remarks and provide conclusions about symmetric power spectra. In Sec. VI, we state possible experimental applications to test single-site addressability with resonance fluorescence measurements. Finally, we give our conclusions in Sec. VII.

II. HAMILTONIAN AND MASTER EQUATION

In our model, we consider N identical two-level atoms at fixed positions \mathbf{r}_μ and define the distances $\mathbf{R}_{\mu\nu} = \mathbf{r}_\mu - \mathbf{r}_\nu$. We demand, however, that all atoms lie inside a 2D plane, which we refer to as the atomic plane. The ground state of atom μ is denoted by $|g_\mu\rangle$, and the excited state is denoted by $|e_\mu\rangle$, where $\mu = 1, 2, \dots, N$ labels the atoms. Apart from the laser that illuminates them, the atoms couple to all modes of the quantized electromagnetic vacuum. The time evolution of

^{*}peter.degenfeld-schonburg@ph.tum.de

the atomic system, therefore, can be described by the master equation [13],

$$\begin{aligned} \partial_t \rho(t) &= \mathbf{L}(\rho(t)) = -\frac{i}{\hbar} [H, \rho(t)] + \frac{\gamma}{2} \sum_{\mu=1}^N [2\sigma_{\mu}^{-} \rho(t) \sigma_{\mu}^{+} \\ &\quad - \sigma_{\mu}^{+} \sigma_{\mu}^{-} \rho(t) - \rho(t) \sigma_{\mu}^{+} \sigma_{\mu}^{-}] + \sum_{\substack{\mu, \nu=1 \\ \mu \neq \nu}}^N \Gamma^{\mu\nu} [2\sigma_{\nu}^{-} \rho(t) \sigma_{\mu}^{+} \\ &\quad - \sigma_{\mu}^{+} \sigma_{\nu}^{-} \rho(t) - \rho(t) \sigma_{\mu}^{+} \sigma_{\nu}^{-}], \end{aligned} \quad (1)$$

with Liouvillian $\mathbf{L}(\cdot)$, where the operators $\sigma_{\mu}^{+} = |e_{\mu}\rangle\langle g_{\mu}|$ ($\sigma_{\mu}^{-} = |g_{\mu}\rangle\langle e_{\mu}|$) create (destroy) an excitation in the μ th atom. The decay rate γ accounts for the spontaneous emission from a single atom, whereas, the collective damping rates $\Gamma^{\mu\nu} = \Gamma^{\nu\mu}$ account for the decay of the collective atomic states. Since the spatial separation of the atoms in our setup is about $1/2$ of the wavelength corresponding to the atomic transition, the often-used assumption of independent quantum environments [14,15] for the individual atoms is not justified in our paper. Consequently, the collective decay processes associated with $\Gamma^{\mu\nu}$ are indeed important [16]. This also is confirmed by our results.

The unitary part of the time evolution of the reduced density matrix $\rho(t)$ is governed by the Hamiltonian,

$$H = H_0 + H_L + H_{dd}, \quad (2)$$

consisting of three parts: the bare atomic part H_0 , the laser-atom coupling H_L , and the dipole-dipole interaction potential H_{dd} . In a frame that rotates with the frequency ω_L of the driving laser, the bare Hamiltonian,

$$H_0 = \frac{\hbar\Delta}{2} \sum_{\mu=1}^N \sigma_{\mu}^z = \frac{\hbar\Delta}{2} \sum_{\mu=1}^N (|e_{\mu}\rangle\langle e_{\mu}| - |g_{\mu}\rangle\langle g_{\mu}|) \quad (3)$$

is determined by the detuning $\Delta = \omega_0 - \omega_L$, where ω_0 is the frequency of the atomic transition. The laser-atom coupling, in turn, depends on the Rabi frequency,

$$H_L = \hbar \sum_{\mu=1}^N \Omega_{\mu} (\sigma_{\mu}^{+} + \sigma_{\mu}^{-}). \quad (4)$$

The atoms are driven by a laser traveling perpendicular to the atomic plane. Hence, the laser field at each atom has the same phase. Without loss of generality, we, thus, choose Ω_{μ} to be real and positive for all atoms. We consider a Gaussian beam profile focused onto the atomic plane and model the field amplitude at the position of the μ th atom by the Rabi frequency,

$$\Omega_{\mu} \equiv \Omega(\mathbf{r}_{\mu}) = \Omega_0 e^{-4(\ln 2)(\mathbf{r}_{\mu}^2/\eta^2)}, \quad (5)$$

where $\Omega_0 \in \mathbb{R}$ represents the intensity at the center of the beam, which defines the point of origin with a FWHM of η ; see Fig. 1. This definition is consistent with our notion of

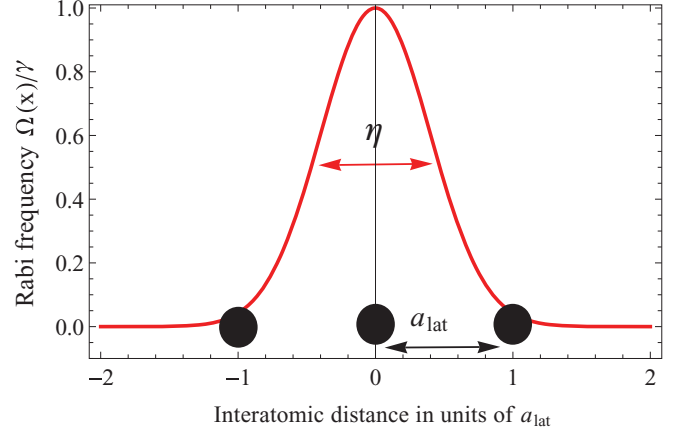


FIG. 1. (Color online) Notion of single-site addressing in an optical lattice. The atoms are fixed in the lattice sites while a laser beam traveling perpendicular to the interatomic axis is focused onto one site. The beam profile is given by a Gaussian envelope with a FWHM η as given in Eq. (5). The parameters a_l and η match the experimental parameters of Ref. [9].

single-site addressing, pictured in Fig. 1, which is motivated by the optical-lattice experiments [8–10] with single-atom occupation on one lattice site and where the central atom is addressed by a focused Gaussian laser beam. In our model, we assume the atoms to be stationary during the illumination process, i.e., we consider a lattice in the Mott-insulator regime.

The coupling to the electromagnetic vacuum induces a dipole-dipole interaction between the atoms due to a mutual exchange of photons. This dipole-dipole interaction arises in the derivation process of the master equation. Similar to the collective damping rate, it is a consequence of the fact that all atoms couple to the same quantum environment.

The dipole-dipole interaction $J^{\mu\nu}$, which should not be confused with the interaction between two static dipoles, is the coherent counterpart to the incoherent collective damping rate $\Gamma^{\mu\nu}$. The operator form of the dipole-dipole Hamiltonian can be taken to read

$$H_{dd} = \hbar \sum_{\substack{\mu, \nu=1 \\ \mu \neq \nu}}^N \frac{J^{\mu\nu}}{2} (\sigma_{\mu}^{+} \sigma_{\nu}^{-} + \sigma_{\nu}^{+} \sigma_{\mu}^{-}), \quad (6)$$

with interaction strength $J^{\mu\nu} = J^{v\mu}$, which depends on only two parameters. Namely, the distance $|\mathbf{R}_{\mu\nu}|$ between the atoms and the angle $\alpha^{\mu\nu} = \angle(\mathbf{R}_{\mu\nu}, \vec{d}_0)$ between the interatomic separation vector and the dipole moment \vec{d}_0 of the atoms. By introducing the dimensionless quantity $x^{\mu\nu} := \frac{|\mathbf{R}_{\mu\nu}|}{\lambda_0}$, where λ_0 is the wavelength corresponding to the energy splitting ω_0 , we find the following form for the dipole-dipole interaction:

$$\begin{aligned} J^{\mu\nu}(\alpha^{\mu\nu}, x^{\mu\nu}) &= \frac{3}{4} \gamma \left\{ [\cos^2(\alpha^{\mu\nu}) - 1] \frac{\cos(2\pi x^{\mu\nu})}{2\pi x^{\mu\nu}} + [1 - 3 \cos^2(\alpha^{\mu\nu})] \right. \\ &\quad \left. \times \left[\frac{\sin(2\pi x^{\mu\nu})}{(2\pi x^{\mu\nu})^2} + \frac{\cos(2\pi x^{\mu\nu})}{(2\pi x^{\mu\nu})^3} \right] \right\}, \end{aligned} \quad (7)$$

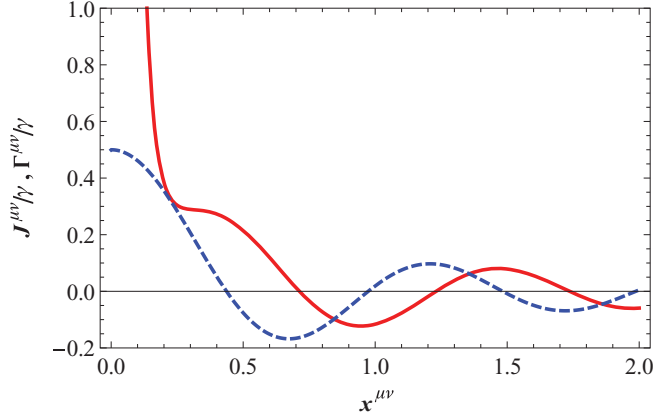


FIG. 2. (Color online) The dipole-dipole interaction $J^{\mu\nu}$ (solid red line) and the collective damping rate $\Gamma^{\mu\nu}$ (blue dashed line) in units of γ as a function of the interatomic separation $x^{\mu\nu}$ with $\alpha^{\mu\nu} = \frac{\pi}{2}$.

and for the collective damping rate,

$$\begin{aligned} \Gamma^{\mu\nu}(\alpha^{\mu\nu}, x^{\mu\nu}) &= \frac{3}{4}\gamma \left\{ [1 - \cos^2(\alpha^{\mu\nu})] \frac{\sin(2\pi x^{\mu\nu})}{2\pi x^{\mu\nu}} + [1 - 3\cos^2(\alpha^{\mu\nu})] \right. \\ &\quad \left. \times \left[\frac{\cos(2\pi x^{\mu\nu})}{(2\pi x^{\mu\nu})^2} - \frac{\sin(2\pi x^{\mu\nu})}{(2\pi x^{\mu\nu})^3} \right] \right\} \end{aligned} \quad (8)$$

given in units of the spontaneous emission rate $\gamma = \frac{\omega_0^3 |\vec{d}_0|^2}{3\pi\epsilon_0\hbar c^3}$. Both quantities decay asymptotically as $\sim \frac{1}{x^{\mu\nu}}$; see Fig. 2, which indicates that the spectral properties of many atoms separated by a large distance do not differ from the spectral properties of a single atom. In order to find collective dynamics, the interatomic distances, at least, should be on the order of the atomic wavelength, i.e., $x^{\mu\nu} \lesssim 1$. On these small length scales, addressing a single atom becomes challenging. We show that the collective quantities affect the spectral response of the atoms and reveal whether single-atom addressing takes place or not.

III. SPECTRUM OF RESONANCE FLUORESCENCE

In the following, we focus on the spectral distribution of the fluorescence light emitted by the atoms in the steady-state limit. First, we concentrate on the total steady-state intensity, which is given by the normally ordered one-time correlation function of the emitted electric field [17],

$$I_{ss}(\mathbf{r}) = \lim_{t \rightarrow \infty} \langle \hat{\mathbf{E}}^{(-)}(\mathbf{r}, t) \cdot \hat{\mathbf{E}}^{(+)}(\mathbf{r}, t) \rangle. \quad (9)$$

Here, $\hat{\mathbf{E}}^{(+)}$ ($\hat{\mathbf{E}}^{(-)}$) denotes the positive (negative) frequency part of the field operator, which is related to the atomic transition operator σ_{μ}^{-} by [18]

$$\hat{\mathbf{E}}^{(+)}(\mathbf{r}, \hat{t}) = -\frac{\omega_0^2 \hat{\mathbf{r}} \times (\hat{\mathbf{r}} \times \vec{d}_0)}{4\pi\epsilon_0 c^2 r} \sum_{\mu=1}^N \sigma_{\mu}^{-}(\hat{t}) e^{-ik_0 \hat{\mathbf{r}} \cdot \mathbf{r}_{\mu}}, \quad (10)$$

with the retarded time $\hat{t} = t - \frac{r}{c}$ at a point $\mathbf{r} = r\hat{\mathbf{r}}$ in the far-field zone. The physical picture here is that every photon that is annihilated in the detection process had to be emitted

by an atom at an earlier time \hat{t} . Turning back to the spectral properties of the atoms, we introduce the so-called power spectrum. It displays the emitted fluorescence intensity per energy interval and is given by the Fourier transform of the two-time correlation function of the electric field,

$$S_{ss}(\mathbf{r}, \omega) = \lim_{t \rightarrow \infty} \int_{-\infty}^{\infty} \frac{d\tau}{2\pi} e^{-i\omega\tau} \langle \hat{\mathbf{E}}^{(-)}(\mathbf{r}, t + \tau) \cdot \hat{\mathbf{E}}^{(+)}(\mathbf{r}, t) \rangle. \quad (11)$$

By making use of Eq. (10), the power spectrum can be expressed in terms of atomic two-time correlation functions,

$$\begin{aligned} S_{ss}(\mathbf{r}, \omega) &= S_0(\mathbf{r}) \lim_{t \rightarrow \infty} \sum_{\mu, \nu=1}^N \text{Re} \left\{ \int_0^{\infty} d\tau e^{-i(\omega - \omega_L)\tau} \right. \\ &\quad \left. \times \langle \sigma_{\mu}^{+}(t + \tau) \sigma_{\nu}^{-}(t) \rangle e^{ik_0 \hat{\mathbf{r}} \cdot (\mathbf{r}_{\mu} - \mathbf{r}_{\nu})} \right\}, \end{aligned} \quad (12)$$

where $\text{Re}\{\cdot\}$ denotes the real part and $S_0(\mathbf{r}) = \frac{I_0(\mathbf{r})}{\pi} = \frac{1}{\pi} \left| \frac{\omega_0^2 \hat{\mathbf{r}} \times (\hat{\mathbf{r}} \times \vec{d}_0)}{4\pi\epsilon_0 c^2 r} \right|^2$ denotes a normalization factor that contains the radiation properties of a dipole. The factor $e^{i\omega_L \tau}$ arises from the fact that we work in a rotating frame with respect to the operator $\frac{\hbar\omega_L}{2} \sum_{\mu=1}^N \sigma_{\mu}^z$. All the atomic one- and two-time correlation functions are accessible via the master Eq. (1) and by usage of the quantum-regression theorem [19].

To analyze the power spectrum S_{ss} as given in Eq. (12), it is helpful to split the expression into a coherent and an incoherent part. For two operators \hat{A} and \hat{B} , the expectation value of the product $\hat{A}\hat{B}$ always can be separated into a coherent and an incoherent part [3,17],

$$\langle \hat{A}\hat{B} \rangle = \langle \hat{A} \rangle \langle \hat{B} \rangle + \langle (\hat{A} - \langle \hat{A} \rangle) (\hat{B} - \langle \hat{B} \rangle) \rangle, \quad (13)$$

respectively. Therefore, it is clear that the coherent part of the power spectrum is always proportional to a δ function since

$$\begin{aligned} S_{ss}^{co}(\mathbf{r}, \omega) &\propto \lim_{t \rightarrow \infty} \int_{-\infty}^{\infty} d\tau e^{-i(\omega - \omega_L)\tau} \langle \sigma_{\mu}^{+}(t + \tau) \rangle \langle \sigma_{\nu}^{-}(t) \rangle \\ &= \langle \sigma_{\mu}^{+} \rangle_{ss} \langle \sigma_{\nu}^{-} \rangle_{ss} \int_{-\infty}^{\infty} d\tau e^{-i(\omega - \omega_L)\tau} \\ &\propto \delta(\omega - \omega_L). \end{aligned} \quad (14)$$

Another feature of the power spectrum for $N \geq 2$ atoms is the geometry dependence arising from the exponential $e^{ik_0 \hat{\mathbf{r}} \cdot (\mathbf{r}_{\mu} - \mathbf{r}_{\nu})}$. For atoms where the collective parameters $\Gamma^{\mu\nu}$ and $J^{\mu\nu}$ are negligible, this interference effect, however, does not contribute to the interesting part of the spectrum, namely, the incoherent part. In this case, the expectation values of $\langle \sigma_{\mu}^{+} \sigma_{\nu}^{-} \rangle$ always factorize for $\mu \neq \nu$, and the interference terms only enter the coherent part of the spectrum. This results in an incoherent part of the spectrum that is the sum of single-atom Mollow spectra. In cases where $\Gamma^{\mu\nu}$ and $J^{\mu\nu}$ are not negligible, the interference terms enter the incoherent part of the spectrum and can make it asymmetric. This effect can serve as a signature of single-site addressing and lies at the center of our investigations.

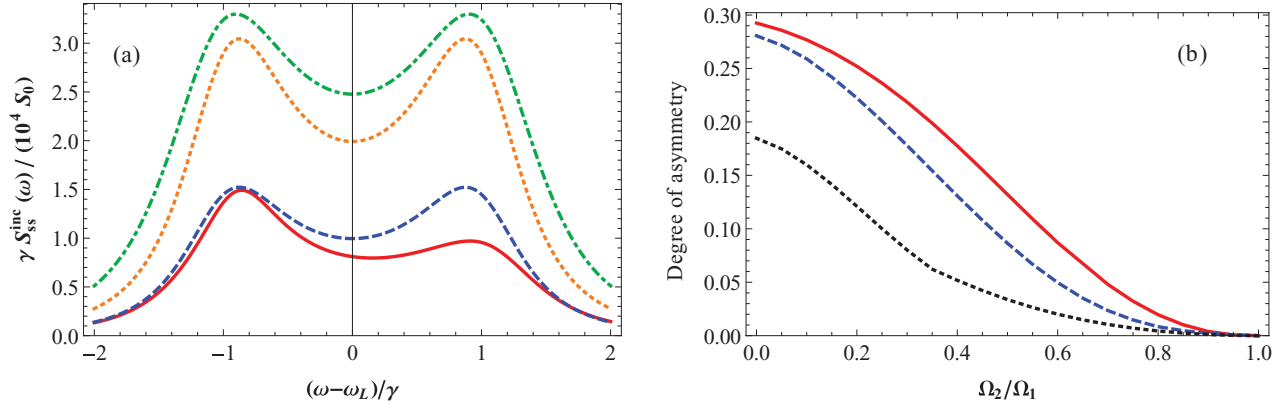


FIG. 3. (Color online) (a) Incoherent part of the power spectrum for two atoms with $\mathbf{R}_{21} = a_l \vec{e}_x = 0.82\lambda_0 \vec{e}_x$, $\alpha^{12} = \pi/2$, $J^{12} \approx -0.09\gamma$, $\Gamma^{12} \approx -0.11\gamma$, $\Delta = \gamma$, $\sigma = 600$ nm, and $\Omega_1 = 0.1\gamma$. The detector is positioned in the xy plane with $\theta = \angle(\hat{\mathbf{r}}, \mathbf{R}_{21}) \approx 0.92$. The solid red and dashed blue lines display the spectrum under single-atom addressing, i.e., $\Omega_2 \approx 0.004\Omega_1 \approx 0$, whereas, the dot-dashed green and dotted orange lines consider a broad laser beam with $0.1\gamma = \Omega_1 \approx \Omega_2$. The dashed blue and the dotted orange lines, however, display the case where the collective parameters $J^{\mu\nu}$ and $\Gamma^{\mu\nu}$ artificially have been set to zero. (b) The degree of asymmetry as defined in Eq. (15) plotted as a function of the ratio Ω_2/Ω_1 for parameters as in (a) except for $\Omega_1 = 0.1\gamma \approx |J^{12}| \approx |\Gamma^{12}|$ (solid red line), $\Omega_1 = 0.5\gamma \approx 5|J^{12}| \approx 5|\Gamma^{12}|$ (dashed blue line), and $\Omega_1 = 1\gamma \approx 10|J^{12}| \approx 10|\Gamma^{12}|$ (dotted black line).

IV. BREAKDOWN OF SPECTRAL SYMMETRY

A. Two atoms

To explain the basic physical mechanisms behind our results, it is convenient to concentrate on the spectrum of two atoms first. The position of atom 1 defines the point of origin, i.e., $\mathbf{r}_1 = \{0, 0, 0\}^\top$. Atom 2 is just positioned in the next lattice site at $\mathbf{r}_2 = \{a_l, 0, 0\}^\top$. For the lattice constant and the FWHM of the laser beam, we choose $a_l = 640$ and $\sigma = 600$ nm, such as in Ref. [9]. The dipole moments are oriented along the z axis $\vec{d}_0 \propto \vec{e}_z$, which leads to $\alpha^{12} = \pi/2$. For the D_2 transition of ^{87}Rb (transition wavelength $\lambda_0 = 780$ nm), the collective parameters result in $\Gamma^{12} \approx -0.11\gamma$ and $J^{12} \approx -0.09\gamma$.

Figure 3(a) compares the case of a broad laser beam, i.e., $\Omega_1 = \Omega_2 = 0.1\gamma$, to the case of a laser beam with a FWHM of $\sigma = 600$ nm focused onto atom 1, which results in $\Omega_1 = 0.1\gamma \approx 25\Omega_2$. We refer to the latter case as single-site addressing. It is seen that the spectral symmetry breaks down in the case of single-site addressing under the effect of the dipole-dipole interaction. For two atoms that are illuminated with equal intensity, we find a spectrum of symmetric Mollow shape as shown in Fig. 3(a), see dot-dashed green line. Under single-site addressing, however, the peak on the right-hand side of the spectrum is suppressed, which leads to an asymmetry, see the solid red line. To illustrate that this effect can be attributed to the presence of the dipole-dipole interaction J^{12} and the collective damping rate Γ^{12} , we compare our results to the physically rather impossible situation where the collective parameters Γ^{12} and J^{12} are turned off artificially. As expected, we find the symmetric Mollow spectrum, dashed blue curve for one atom being illuminated and dotted orange curve for two atoms. The latter only shows little deviations in the peak heights and positions from the cases of $\Omega_1 = \Omega_2$ and $J^{12} \neq 0$, $\Gamma^{12} \neq 0$.

Note that only two peaks out of the triplet (at $\pm\Delta$) can be seen because of the weak driving strength $\Omega_0 = 0.1\gamma$ with Ω_0

as defined in Eq. (5). We choose such a weak Rabi frequency because the effect of symmetry breaking in the spectrum is more evident if the Rabi frequency is on the order of the dipole-dipole interaction. In the case where $\Omega_0 \gg J^{\mu\nu}$, the dipole-dipole interaction is just a small perturbation to the driving of a single two-level atom, hence, the symmetric Mollow shape dominates the spectrum.

Figure 3(b) displays the degree of asymmetry in the spectra for different ratios of $\frac{\Omega_2}{\Omega_1}$, which is equivalent to different FWHMs of the laser beam. We consider here a degree of asymmetry, which is defined as

$$D = \frac{1}{S_{\max}} [\max\{|S(\tilde{\omega}) - S(-\tilde{\omega})| : \tilde{\omega} = \omega - \omega_L > 0\}], \quad (15)$$

normalized to the highest intensity S_{\max} in the spectrum,

$$S_{\max} = \max\{S(\tilde{\omega}) : \tilde{\omega} = \omega - \omega_L \in \mathbb{R}\}. \quad (16)$$

For parameters as in Fig. 3(a), the definition of the degree of asymmetry corresponds to the visibility of the difference in the peak heights. One can see that the degree of asymmetry decreases monotonically with increasing ratios of $\frac{\Omega_2}{\Omega_1}$ and goes exactly to zero as $\Omega_2 \rightarrow \Omega_1$. Furthermore, the degree of asymmetry is highest if the Rabi frequency is comparable to the dipole-dipole interaction J^{12} between the atoms.

In conclusion, the degree of asymmetry in the spectrum is a signature for the degree of single-site addressing, provided that the collective parameters $J^{\mu\nu}$ and $\Gamma^{\mu\nu}$ are on the order of the driving strength. Therefore, we emphasize that single-atom addressing in the regime of large interatomic separations certainly is not challenging, but for small interatomic separations, the collective atomic properties reveal whether single-site addressing occurs in the system.

Our results also give direct evidence that the dipole-dipole interaction $J^{\mu\nu}$ is induced by the mutual exchange of photons between the atoms. Indeed, as already mentioned, the incoherent part of the spectrum only contains the interference of light emitted from separate atoms if the dipole-dipole

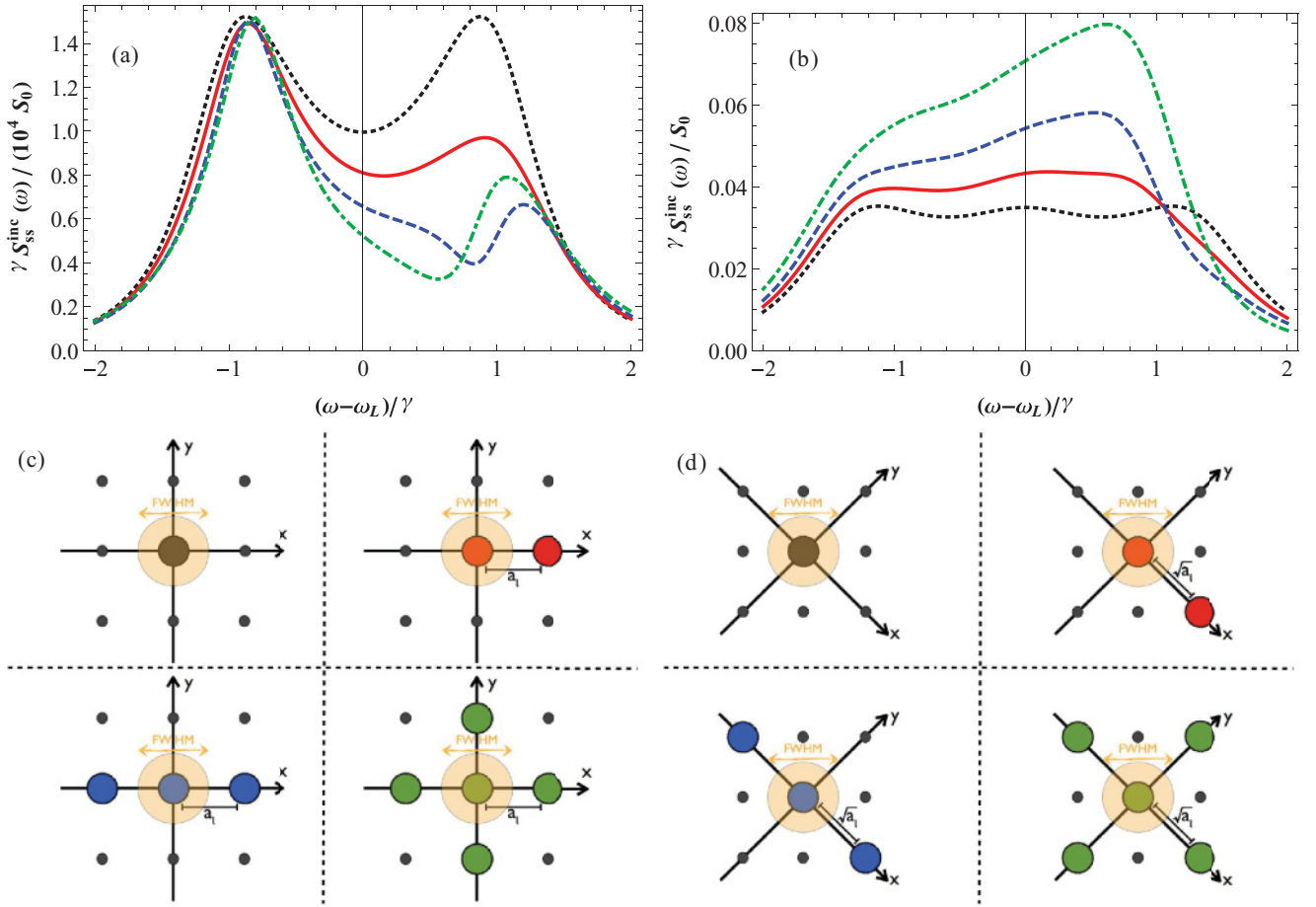


FIG. 4. (Color online) Incoherent part of the power spectrum (a) and (b) with the corresponding atomic configurations in the lattice below (c) and (d), respectively. (a) Incoherent part of the power spectrum with parameters as in Fig. 3(a). The solid red curve shows the spectrum for two atoms under single-atom addressing just as the solid red line in Fig. 3(a). The dashed blue curve displays the spectrum of three atoms where the third atom is placed at $\mathbf{r}_3 = -a_l \vec{e}_x$. This represents single-site addressing in a 1D optical lattice where the contributions of the nearest neighbors of the addressed atom are taken into account. For the 2D lattice, we place two more atoms at $\mathbf{r}_4 = a_l \vec{e}_y$ and $\mathbf{r}_5 = -a_l \vec{e}_y$ and find very similar features (dot-dashed green curve). The Mollow spectrum of a single atom also is given for comparison (dotted black curve). (b) Incoherent part of the power spectrum for two atoms (solid red curve), three atoms (dashed blue curve), and five atoms (dot-dashed green curve) with the parameters $\Delta = \gamma$ and $\Omega_0 = 0.5\gamma$. The positions of the atoms are $\mathbf{r}_1 = \{0, 0, 0\}^T$, $\mathbf{r}_2 = a_l \{\sqrt{2}, 0, 0\}^T$, $\mathbf{r}_3 = a_l \{-\sqrt{2}, 0, 0\}^T$, $\mathbf{r}_4 = a_l \{0, \sqrt{2}, 0\}^T$, and $\mathbf{r}_5 = a_l \{0, -\sqrt{2}, 0\}^T$ as illustrated in the picture below with $a_l = 532$ and $\sigma = 700$ nm as in Refs. [8,10]. The detector is positioned in the far-field zone at $\hat{\mathbf{r}} = \hat{r}\{0, 1, 0\}$. All the lines consider single-site addressing, which is compared to the Mollow line (dotted black curve). In (c) and (d), small black dots indicate lattice sites, colored dots indicate the atoms considered for plots of the corresponding color in (a) and (b), respectively, and the faint orange circle indicates the FWHM of the probe laser.

interaction $J^{\mu\nu}$ is finite. Yet the interference effect is still present even if atom 2 is not illuminated by the laser at all, i.e., $\Omega_2 = 0$. This indicates that processes where atom 1 absorbs a photon from the laser field that emits a photon that travels to atom 2 where it is absorbed and is emitted again must exist. Since we look at the spectrum in the steady-state limit and the Rabi frequency Ω_0 is comparable to J^{12} , these processes occur at a rate large enough to generate the observed interference in the spectral light of the atomic ensemble. Note that this interference is not due to coherent classical light, but it is rather of quantum-mechanical nature.

B. Larger numbers of atoms

If one considers the investigation of single-site addressing in a 1D or 2D optical lattice, more than one neighboring

atom should be taken into account. Since the dipole-dipole interaction and the collective damping rates decay as $\frac{1}{x^{\mu\nu}}$ with increasing separation $x^{\mu\nu}$, one, however, can obtain estimates for larger lattices by just considering a limited number of lattice sites or rather atoms contributing to the spectrum. We study the effects of single-site addressing in a 1D and 2D optical lattice up to a level where the atoms with the highest contribution to the spectrum are taken into account. These atoms are the ones where the dipole-dipole interaction potential $J^{1\mu}$ between the μ th atom and the addressed atom is largest in magnitude.

Figure 4 displays the impact of single-site addressing in a 1D optical lattice (dashed blue curve) and a 2D optical lattice (dot-dashed green curve) configuration within the approximation described above and compares it to the case of two atoms (solid red curve) and to the Mollow spectrum of a single atom (black dotted curve). In part (a) of Fig. 4,

we have chosen parameters for the lattice constant and the FWHM of the laser beam, such as in Ref. [9], i.e., $a_l = 640$ and $\sigma = 600$ nm. For this lattice constant, the magnitude of the dipole-dipole interaction is largest between the addressed atom positioned at $\mathbf{r}_1 = \{0,0,0\}^\top$ and the nearest neighbors in the lattice, hence, the atoms positioned at $\mathbf{r} = \{\pm a_l, 0, 0\}^\top$ and $\mathbf{r} = \{0, \pm a_l, 0\}^\top$. The parameters $\Delta = \gamma$ and $\Omega_1 = 0.1\gamma$ coincide with the parameters chosen in Fig. 3. Again, the detector is positioned in the xy plane with $\theta = \angle(\hat{\mathbf{r}}, \mathbf{R}_{21}) \approx 0.92$. Therefore, the solid red line in Fig. 4(a) is the same as the solid red line in Fig. 3(a). It shows the incoherent part of the output spectrum for the addressed atom at $\mathbf{r}_1 = \{0,0,0\}^\top$ in the presence of another atom at $\mathbf{r} = \{a_l, 0, 0\}^\top$. The dashed blue line displays the same situation but with a third atom placed at $\mathbf{r} = \{-a_l, 0, 0\}^\top$. The dot-dashed green line shows the spectrum if a fourth and a fifth atom are placed at $\mathbf{r} = \{0, \pm a_l, 0\}^\top$. In all cases, we find a broken spectral symmetry under single-site addressing. The peak on the right-hand side is suppressed for all atomic configurations as compared to the single-atom Mollow spectrum. We also note that spacial symmetry of the atomic setup does not lead to spectral symmetry of the emitted light.

Figure 4(b) displays the same situation as Fig. 4(a) but with lattice parameters as in the experiments of Refs. [8,10]. The lattice constant in the experiment is equal to 532 nm. This leads to a dipole-dipole interaction of $J^{\mu\nu} \approx 0.03\gamma$ between atoms positioned in two adjacent lattice sites, whereas, atoms separated by $\sqrt{2}a_l$ have a dipole-dipole interaction of $J^{\mu\nu} \approx -0.12\gamma$. Hence, in our numerical calculations, we concentrate on the contributions from these atoms and neglect the contributions from the nearest neighbors of the addressed atom. Although the breaking of spectral symmetry is displayed in Fig. 4(b) as well, we notice that the overall intensity of the case with a finite dipole-dipole interaction is a bit larger than for a single atom. Figure 4(a) exhibits the opposite behavior. This effect mainly is due to the different positionings of the detector in Figs. 4(a) and 4(b).

If the atoms in the configurations of Figs. 4(c) and 4(d) all are driven by the same driving strength, we find symmetric power spectra in all cases. In the case of two atoms, the degree of asymmetry is exactly zero. In the cases of three or five atoms, we find a degree of asymmetry, which is negligible but is not exactly zero. For two equally driven atoms, the master equation is fully symmetric under the exchange of these two atoms. This is no longer true in the case of three or five equally driven atoms as, for example, $J^{12} \neq J^{23}$ because of the geometry dependence of the dipole-dipole interaction. However, if we choose $J^{\mu\nu} \equiv J$ and $\Gamma^{\mu\nu} \equiv \Gamma$ for all $\mu, \nu \in \{1, \dots, N\}$ artificially and drive all atoms with the same Rabi frequency, we find a spectrum for two, three, four, or five atoms with a degree of asymmetry that is exactly zero. In the next section, we discuss this observation further.

V. SOME CONCLUSIONS AND REMARKS ABOUT THE SYMMETRY OF THE SPECTRA

Our results lead us to a remarkable first conclusion, regarding our particular system:

(1) In the case where the master equation and, therefore, the density matrix are fully symmetric under the exchange of each

possible pair of two-level atoms μ and ν (i.e., under atomic permutation), the total spectrum of emission of the system is symmetric around the laser frequency.

Moreover, putting together these results with many other examples, one could think of [20], we further envision a second conclusion regarding any open quantum system (QS) in general:

(2) Provided that a single QS (such as a few-level system or harmonic oscillator under coherent or incoherent continuous excitation) exhibits a symmetric steady-state power spectrum, then a number N of such QSs coupled to each other, in a way that the density matrix is fully symmetric under all possible permutations of these QSs, also exhibits a symmetric total steady-state power spectrum. Consequently, all possible auto- and cross-correlation functions between pairs of QSs will be real and, therefore, experimentally observable.

The second conclusion is a generalization of the first one. These statements are difficult to prove starting from the properties of the Liouvillian of an ensemble of coupled QSs. Here, we only explore some directions that such a proof may take.

The power spectrum for N QSs with associated operator σ_μ consists of a sum of N^2 contributions $S_{\mu\nu}(\tilde{\omega})$, each given by

$$S_{\mu\nu}(\tilde{\omega}) \propto \text{Re} \left\{ \int_0^\infty d\tau e^{-i\tilde{\omega}\tau} \langle \sigma_\mu^+(\tau) \sigma_\nu^-(\tau) \rangle_{ss} \right\}, \quad (17)$$

with $\langle \sigma_\mu^+(\tau) \sigma_\nu^-(\tau) \rangle_{ss} = \lim_{t \rightarrow \infty} \langle \sigma_\mu^+(t + \tau) \sigma_\nu^-(t) \rangle$ and $\tilde{\omega} = \omega - \omega_L$. Each of these terms can be decomposed into a symmetric and an asymmetric part simply by separating the corresponding correlator into its real and imaginary parts,

$$\begin{aligned} S_{\mu\nu}(\tilde{\omega}) &= S_{\mu\nu}^{\text{sy}}(\tilde{\omega}) + S_{\mu\nu}^{\text{asy}}(\tilde{\omega}) \\ &= \int_0^\infty d\tau \text{Re} \{ \langle \sigma_\mu^+(\tau) \sigma_\nu^-(\tau) \rangle_{ss} \} \cos(\tilde{\omega}\tau) \\ &\quad - \int_0^\infty d\tau \text{Im} \{ \langle \sigma_\mu^+(\tau) \sigma_\nu^-(\tau) \rangle_{ss} \} \sin(\tilde{\omega}\tau). \end{aligned} \quad (18)$$

In the case where the master equation and, therefore, the density matrix are fully symmetric under QS permutation, we have $S_{\mu\nu}(\tilde{\omega}) = S_{\nu\mu}(\tilde{\omega})$. Consequently, the total spectrum can be computed in terms of two different correlators only, for example,

$$S(\tilde{\omega}) = N S_{11}(\tilde{\omega}) + N(N-1) S_{12}(\tilde{\omega}). \quad (19)$$

In this case, the spectrum is symmetric if and only if every correlator $\langle \sigma_\mu^+(\tau) \sigma_\nu^-(\tau) \rangle_{ss}$ is real. Then, the two-time operator $\sigma_\mu^+(\tau) \sigma_\nu^-(\tau)$ with $\mu \neq \nu$ becomes an observable in the steady state as we stated in our second conclusion.

However, the fact that the correlators become real when the spectrum is symmetric does not provide new information about the system; it is only a mathematical implication. The general question when an open quantum system should have a symmetric spectrum around some relevant frequency (the laser in the case of coherent excitation) is not a trivial one. First, this depends crucially on the nature of the excitation that is being detected, that is, the operators appearing in the two-time correlator. In our case generalized for N atoms, we refer to the collective Dicke operator $\sigma_S^\pm = \sum_{\mu=1}^N \sigma_\mu^\pm$,

but it could be any deexcitation operator in the system that corresponds to some physical entity. Each peak that appears in the spectrum is related to the *probability amplitude* to transit between two eigenstates of the system by emitting one of these quasiparticles. This means that both the dynamics of the dressed states and their quasiparticle components play a role. In order to make this link clearer, let us decompose the incoherent part of a spectrum into a sum of d^2 peaks [20],

$$S(\tilde{\omega}) = \frac{1}{\pi} \sum_{p=1}^{d^2} \left[\frac{L_p \gamma_p / 2 - K_p (\tilde{\omega} - \omega_p)}{(\gamma_p / 2)^2 + (\tilde{\omega} - \omega_p)^2} \right], \quad (20)$$

with ω_p and γ_p (peak position and linewidth), L_p and K_p (Lorentzian and dispersive weights) as all real parameters, and d as the dimension of the Hilbert space. Then, $-(i\omega_p + \gamma_p/2)$ are the eigenvalues of the Liouvillian in matrix form \mathbf{L} , which are either real (giving rise to a single Lorentzian peak at the center) or pairs of complex conjugates (giving rise to a pair of sister peaks symmetrically placed around the center, with equal broadening) [21].

A given pair of sister peaks (with $i\omega_\alpha + \gamma_\alpha/2 = -i\omega_\beta + \gamma_\beta/2$) is symmetric if the complex weights are also conjugates,

$$L_\alpha + iK_\alpha = L_\beta - iK_\beta. \quad (21)$$

These are computed from the eigenvectors of \mathbf{L} including the steady-state density matrix. They correspond exactly to the transition-probability amplitude as mentioned above. The balance between two amplitudes gives rise to a pair of symmetric twin peaks. If this is the case for all sister peaks, the total spectrum, of course, is symmetric.

In order to grasp all the physical senses of this balance condition, one would need to identify (or rather to reconstruct) the eigenstates of the system under study. This is not an easy task, especially in the presence of both dissipation and excitation [22,23]. In some limiting cases, however, such as one strongly driven two-level system, it is possible [24,25]. The eigenvectors of the full Liouvillian correspond in good approximation to the so-called *dressed states* $|\pm\rangle$ obtained from diagonalizing the Hamiltonian part only. As in this regime, the three peaks that form the Mollow structure are well separated, the interference part of the spectrum is negligible ($K_p \approx 0$), and the condition for symmetry of the two side peaks $L_\alpha = L_\beta$ is equivalent completely to the so-called *detailed balance* between the dressed states: $\rho_{++}\mathcal{P}_{(+ \rightarrow -)} = \rho_{--}\mathcal{P}_{(- \rightarrow +)}$, where $\rho_{\pm\pm}$ are the dressed-state steady-state populations and $\mathcal{P}_{(\pm \rightarrow \mp)}$ are the transition rates between them. On the other hand, if the excitation is weak and there is an overlap between the peaks of the spectrum, dressed states are not the eigenstates of the full Liouvillian anymore, and their detailed balance is no longer a necessary condition for symmetry (in fact, it breaks down out of resonance where the spectrum is still symmetric).

A symmetric spectrum, thus, implies that the probability amplitudes of transitions between eigenstates are balanced. However, the challenging task of reconstructing such eigenstates makes it difficult to foresee and to demonstrate when a system exhibits a symmetric spectrum. specially in a configuration where coupling strength, decay, and excitation rates are on the same order of magnitude as in this paper. Setting Eq. (21) in terms of the eigenvectors of the Liouvillian

gives the mathematical condition that they must fulfill so that the spectrum is symmetric. But this does not bring any further insight into the matter if one cannot identify which properties of the system cause the weights K_α and L_α of the corresponding Liouvillian \mathbf{L} to fulfill this equation.

On the other hand, our conclusions 1 and 2 are somehow intuitive and are expected if one reasons on physical grounds, so let us end this section with a plausible explanation for the symmetry of the spectrum and its breakdown in our particular case.

In our configuration, the QS is simply a two-level atom driven by a laser, whose Mollow spectrum is indeed always symmetric (in the absence of incoherent pumping, pure dephasing or other decoherence effects). When assembling N of such identical and identically driven QSs, new collective states are expected to appear. In this case, the driving is restricted to the set of states $|0\rangle \leftrightarrow \sigma_S^+|0\rangle \leftrightarrow \dots \leftrightarrow (\sigma_S^+)^N|0\rangle$ that form an $(N+1)$ -level system. The remaining nonsymmetric states are not driven at all but provide an effective decay channel for the $(N+1)$ -level system. From dressed-state arguments, it is known that the total spectrum of a coherently driven $(N+1)$ -level system is symmetric. Additional effective decay through the remaining nonsymmetric states does not break the symmetry of the total spectrum as we calculated in previous sections. Now, if the atoms are not driven equally, the laser does not drive the $(N+1)$ -level system solely but also the transitions between nonsymmetric states. This disrupts the dynamics of the $(N+1)$ -level system and induces decoherence in the form of pure dephasing and an effective incoherent pump. Both elements are well known to break the symmetry in the spectra of coherently driven systems [5,26]. Letting other atomic parameters be different, such as decay rates or detunings, has a similar decoherent impact on the dynamics and the symmetry of the spectrum. We have checked that this is the case for systems consisting of up to five two-level atoms.

VI. EXPERIMENTAL APPLICABILITY

In Sec. IV, our numerical results clearly show the signatures of single-site addressing in resonance fluorescence spectra. To summarize, it can be stated that the spectrum is symmetric around the laser frequency if the atoms are illuminated by a laser with equal strength. If, in contrast, only one atom is addressed, the spectrum becomes asymmetric. Thus, it is possible to measure a fluorescence spectrum and to deduce information about the quality of an addressing scheme.

In optical lattices, a large number of ultracold atoms are trapped. As soon as these atoms are illuminated by light, the atoms heat up unavoidably. The detection methods presented in the experiments [8–10] are all destructive measurements in the sense that the atomic sample is too hot after detecting the atoms. The single-site addressing scheme presented in Ref. [10] is designed in a way that the test for the failure or success of the addressing scheme requires a destructive measurement. Hence, the test and the usage of the addressing scheme have to be carried out in different atomic samples.

Yet, if one makes a resonance fluorescence measurement as pictured in this paper, only a small fraction of atoms will be heated. Atoms positioned at the edges of a 2D lattice, for

example, are well suited to test the addressing laser. After the test of the addressing scheme, the laser can be moved over the lattice to the desired position. The test and the usage of the addressing scheme could be carried out in only one atomic sample.

VII. CONCLUSION

In this paper, we calculated and investigated the resonance fluorescence spectra of two-level atoms under the influence of local addressability. We implemented local addressing by means of a laser beam focused on a single atom in an atomic ensemble. A master equation in a Markovian regime modeled the interaction between the atoms and the surrounding electromagnetic vacuum. Due to small interatomic separations, we had to account for a dipole-dipole interaction between atoms that was induced by the mutual exchange of photons and collective damping processes. With numerical calculations, we demonstrated that the output power spectrum of an atomic ensemble was asymmetric in the case of single-atom addressing. We showed that this effect was generated by the presence of the dipole-dipole interaction due to photon exchange. Our results suggest that resonance fluorescence

measurements could provide sensitive tests for the addressing of individual atoms in 1D or 2D optical lattices. They, thus, also allow predicting emission spectra of 1D optical lattices on the surface of optical nanofibers [27]. Our calculations are valid for any set of two-level quantum systems. The applicability of resonance fluorescence measurements as a test for single-site addressability, therefore, is not restricted to neutral atoms in optical lattices but also applies to quantum dots [28] and color centers in diamonds [29]. Furthermore, we provided some physical and intuitive explanations for the symmetry of the spectrum and its breakdown under single-site addressing. We finally generalized our findings as follows: Provided that a single quantum system exhibits a symmetric steady-state power spectrum, this property also holds for N identical and identically coupled quantum systems.

ACKNOWLEDGMENTS

The authors thank Martin Kiffner for fruitful discussions at an earlier stage of this project. This work is part of the Emmy Noether Project No. HA 5593/1-1 funded by the DFG and was supported by the Alexander von Humboldt Foundation and the DFG-CRC 631.

-
- [1] D. F. Walls and G. Milburn, *Quantum Optics* (Springer, Berlin, 2007).
- [2] M. O. Scully and M. S. Zubairy, *Quantum Optics* (Cambridge University Press, Cambridge, UK, 1997).
- [3] B. R. Mollow, *Phys. Rev.* **188**, 1969 (1969).
- [4] E. del Valle and F. P. Laussy, *Phys. Rev. Lett.* **105**, 233601 (2010).
- [5] E. del Valle and F. P. Laussy, *Phys. Rev. A* **84**, 043816 (2011).
- [6] T. G. Rudolph, Z. Ficek, and B. J. Dalton, *Phys. Rev. A* **52**, 636 (1995).
- [7] J.-T. Chang, J. Evers, M. O. Scully, and M. Suhail Zubairy, *Phys. Rev. A* **73**, 031803 (2006).
- [8] J. F. Sherson, C. Weitenberg, M. Endres, M. Cheneau, I. Bloch, and S. Kuhr, *Nature (London)* **467**, 68 (2010).
- [9] W. S. Bakr, J. I. Gillen, A. Peng, S. Fölling, and M. Greiner, *Nature (London)* **462**, 74 (2009).
- [10] C. Weitenberg, M. Endres, M. Cheneau, P. Schauß, T. Fukuhara, I. Bloch, and S. Kuhr, *Nature (London)* **471**, 319 (2011).
- [11] M. J. Hartmann, G. Mahler, and O. Hess, *Phys. Rev. Lett.* **93**, 080402 (2004).
- [12] M. J. Hartmann and M. B. Plenio, *Phys. Rev. Lett.* **100**, 070602 (2008).
- [13] M. Kiffner, M. Macovei, J. Evers, and C. H. Keitel, *Prog. Opt.* **55**, 85 (2010).
- [14] M. J. Hartmann, *Phys. Rev. Lett.* **104**, 113601 (2010).
- [15] M. J. Hartmann, J. Prior, S. R. Clark, and M. B. Plenio, *Phys. Rev. Lett.* **102**, 057202 (2009).
- [16] H. Zoubi and H. Ritsch, *Phys. Rev. A* **83**, 063831 (2011).
- [17] R. J. Glauber, *Phys. Rev.* **130**, 2529 (1963).
- [18] R. H. Lehmann, *Phys. Rev. A* **2**, 889 (1970).
- [19] M. Lax, *Phys. Rev.* **172**, 350 (1968).
- [20] E. del Valle, *Microcavity Quantum Electrodynamics* (VDM Verlag, Saarbrücken, Germany, 2009).
- [21] Because the density matrix is Hermitian, in vectorial representation, $\vec{\rho}^* = T\vec{\rho}$ where T is some similarity transformation. Therefore, \mathbf{L} and $\mathbf{L}^* = T\mathbf{L}T$ have the same characteristic polynomial with real coefficients.
- [22] E. del Valle, F. P. Laussy, and C. Tejedor, *Phys. Rev. B* **79**, 235326 (2009).
- [23] E. del Valle, *Phys. Rev. A* **81**, 053811 (2010).
- [24] D. F. Walls, H. J. Carmichael, R. F. Gragg, and W. C. Schieve, *Phys. Rev. A* **18**, 1622 (1978).
- [25] C. Cohen-Tannoudji and S. Reynaud, *J. Phys. B* **10**, 345 (1977).
- [26] G. S. Agarwal, *Phys. Rev. Lett.* **37**, 1383 (1976).
- [27] E. Vetsch, D. Reitz, G. Sagué, R. Schmidt, S. T. Dawkins, and A. Rauschenbeutel, *Phys. Rev. Lett.* **104**, 203603 (2010).
- [28] C. Santori and Y. Yamamoto, *Nat. Phys.* **5**, 173 (2009).
- [29] F. Jelezko and J. Wrachtrup, *Phys. Status Solidi A* **203**, 3207 (2006).